13. B. Boettner, L. VanAelst, U. Gaul, personal communication
14. K. Takahashi, T. Matsuo, T. Katsube, R. Ueda, D. Yamamoto, *Mech. Dev.* **78**, 97 (1998).
15. M. Itoh, A. Nagafuchi, S. Moroi, S. Tsukita, *J. Cell Biol.* **138**, 181 (1997).
16. X. Wei, H. M. Ellis, *Mech. Dev.* **100**, 217 (2001).
17. B. R. Stevenson, J. D. Siliciano, M. S. Mooseker, D. A. Goodenough, *J. Cell Biol.* **103**, 755 (1986).
18. M. S. Steinberg, M. Takeichi, *Proc. Natl. Acad. Sci. U.S.A.* **91**, 206 (1994).
19. D. Godt, U. Tepass, *Nature* **395**, 387 (1998).
20. A. Gonzalez-Reyes, D. St Johnston, *Development* **125**, 3635 (1998).
21. D. Fristrom, J. W. Fristrom, in *The Development of* Drosophila melanogaster, M. Bate, A. Martinez Arias, Eds. (Cold Spring Harbor Laboratory Press, Cold Spring Harbor, NY, 1993), vol. 2, pp. 843–896.
22. *Rap1* mutant wing clones expressing α-catenin–GFP (*31*) were generated by heat shocking *y w P{ry$^{+t7.2}$ hsFLP}22; P{UAS-DαC-GFP#3} {arm-GAL4}/+; Rap1$^{P[5709]}$ P{w^{hs} FRT}2A/ P{w^{+}nls-GFP} P{w^{hs} FRT}2A* flies. 24h APF pupae were dissected from the pupal case and directly mounted in Vectashield (Vector Labs, Burlingame, CA), then clones were imaged with a MRC1024 confocal microscope (Bio-Rad). Rap1 was tagged with GFP by generating a genomic rescue construct with GP inserted at the NH_2-terminus of Rap1 (*23*). Imaginal discs and 2-hour APF wings expressing GFP-Rap1 or α-catenin–GFP were fixed in 4% formaldehyde and mounted in Vectashield. Images were collected with a Radiance 2000 confocal microscope (Bio-Rad).
23. A. L. Knox, N. H. Brown, in preparation.
24. D. F. Woods, J. W. Wu, P. J. Bryant, *Dev. Genet.* **20**, 111 (1997).
25. T. B. Chou, N. Perrimon, *Genetics* **144**, 1673 (1996).
26. S. Luschnig, J. Krauss, K. Bohmann, I. Desjeux, C. Nusslein-Volhard, *Mol. Cell* **5**, 231 (2000).
27. D. Fristrom, M. Wilcox, J. Fristrom, *Development* **117**, 509 (1993).
28. H. Oda, T. Uemura, Y. Harada, Y. Iwai, M. Takeichi, *Dev. Biol.* **165**, 716 (1994).
29. M. Takahisa *et al.*, *Genes Dev.* **10**, 1783 (1996).
30. D. F. Woods, P. J. Bryant, *Cell* **66**, 451 (1991).
31. H. Oda, S. Tsukita, *Dev. Genes Evol.* **209**, 218 (1999).
32. We thank P. Bryant, R. Fehon, I. Hariharan, R. Howes, H. Oda, S. Luschnig, M. Takahisa, M. Takeichi, and D. Yamamoto for providing antibodies and fly stocks, and S. Bray, B. Harris, D. St Johnston, and R. White for critically reading the manuscript. We thank J. Overton for technical assistance and the members of our lab for valuable advice. Supported by a Wellcome Trust Senior Fellowship (N.H.B.) and grants from the Association of Commonwealth Universities, the New Zealand Federation of University Women, and Trinity College (A.L.K.).

29 October 2001; accepted 10 January 2002

Role of the Isthmus and FGFs in Resolving the Paradox of Neural Crest Plasticity and Prepatterning

Paul A. Trainor,* Linda Ariza-McNaughton,*† Robb Krumlauf‡

Cranial neural crest cells generate the distinctive bone and connective tissues in the vertebrate head. Classical models of craniofacial development argue that the neural crest is prepatterned or preprogrammed to make specific head structures before its migration from the neural tube. In contrast, recent studies in several vertebrates have provided evidence for plasticity in patterning neural crest populations. Using tissue transposition and molecular analyses in avian embryos, we reconcile these findings by demonstrating that classical manipulation experiments, which form the basis of the prepatterning model, involved transplantation of a local signaling center, the isthmic organizer. FGF8 signaling from the isthmus alters *Hoxa2* expression and consequently branchial arch patterning, demonstrating that neural crest cells are patterned by environmental signals.

The cranial neural crest is a pluripotent migratory cell population that plays a critical role in the construction of the vertebrate head, giving rise to the facial and visceral skeleton, most of the skull bones and connective tissue, and the neurons and glia of the peripheral nervous system (*1–3*). The highly conserved segmental organization of the vertebrate hindbrain into rhombomeres (*4*, *5*) plays a key role in patterning the identity and pathways of neural crest cell migration into the branchial arches (*6–12*). Currently, there is a fundamental paradox in mechanisms that pattern neural crest cells and their derivatives. Noden grafted first-arch neural crest precursors posteriorly to new locations in avian embryos, and these ectopic crest cells gave rise to duplications of first-arch skeletal derivatives, such as the quadrate and Meckel's cartilage. This landmark transposition study (*2*) led to the model that cranial neural crest cells are preprogrammed in the neural tube before their migration and that they passively carry positional information necessary for craniofacial morphogenesis from the neural tube to the periphery. This prepatterning model has shaped the way we think about craniofacial development during the past 18 years and has also been used to explain skeletal duplications observed in null mutations of A-P patterning genes, such as *Hoxa2* and *Hoxa3* (*13–15*). However, recent transposition and lineage tracing experiments contradict the prepatterning model, highlighting the plasticity of rhombomeres and cranial neural crest populations [(*11*, *12*, *16–23*) and reviewed in (*5*)]. These studies suggest an alternative dynamic model, in which neural crest patterning relies on a balance of instructive signals from the hindbrain, maintenance signals from the branchial arch environment, and cell community interactions.

In this study, we performed experiments aimed at understanding and resolving the basis for these conflicting models and results. An often-ignored aspect of Noden's analysis is that posterior transplantations of presumptive frontonasal or presumptive first-arch neural crest both produced the same quadrate and Meckel's cartilage duplications. Hence, the same ectopic structures formed irrespective of the axial origin of the neural crest cells. What links these different transplantations is the probable inclusion of the mid/hindbrain isthmus in the grafted tissue. In recent years, it has become apparent that local inductive centers, such as the mid/hindbrain junction (isthmus), play roles in anterior neural patterning (*24*). Noden used the isthmus as a morphological marker for delineating the neural tissue to be grafted posteriorly (Fig. 1A), and therefore one possible explanation for the conflicting results may relate to the inclusion of a localized signaling center along with neural crest progenitors.

To directly test this idea, we transplanted the isthmus posteriorly in place of rhombomere 4 (r4) in ovo, in stage-matched chick embryos at somite stage 8 to 9 (8-9) (Fig. 1, A through C). The donor isthmus included the mid/hindbrain junction and a small population of cells on both sides of the boundary (Fig. 1A). After 24 to 48 hours of in ovo culture, grafted embryos were assayed for effects on *Hoxa2* expression (Fig. 1, D and E), which is the primary determinant of the second branchial arch neural crest phenotype (*13*, *14*). *Hoxa2* expression in the second branchial arch neural crest was inhibited (Fig. 1E), and this was not due to an absence of migrating neural crest cells, because 1,1'-dioctadecyl-3,3,3',3'-tetramethylindocarbonocyanine perchlorate (DiI) labeling of the transplanted tissue shows that numerous

The Stowers Institute for Medical Research, 1000 East 50th Street, Kansas City, MO 64110, USA, and Division of Developmental Neurobiology, The National Institute for Medical Research, London, UK, NW7 1AX.

*These authors contributed equally to this paper.
†Present address: The Sanger Centre, Wellcome Trust Genome Campus, Hinxton, Cambs CB10 1SA, UK.
‡To whom correspondence should be addressed at The Stowers Institute for Medical Research, 1000 East 50th Street, Kansas City, MO 64110, USA. E-mail: rek@stowers-institute.org

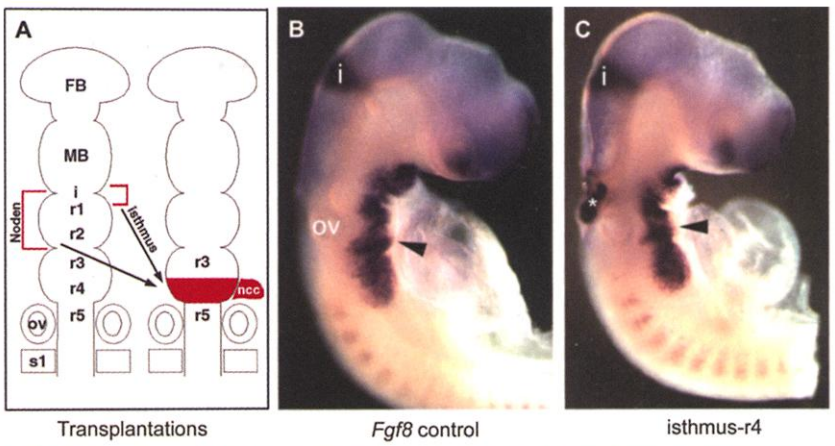

Fig. 1. Transposition of the mid/hindbrain isthmus posteriorly in place of r4 reprograms *Hoxa2* expression in cranial neural crest cells. (**A**) Diagram illustrating transposition. Noden grafted the region from the isthmus to the boundary between r2 and r3. Our isthmus (i) transplantations comprised only the FGF8-expressing territory at the mid/hindbrain junction. In both cases after removal of endogenous r4, the anterior territory containing neural crest cell (ncc) progenitors was transposed posteriorly into the caudal hindbrain at the level of r4 (arrows) FB, forebrain; MB, midbrain; ov, otic vesicle; s1, somite 1. (**B** and **C**) *Fgf8* in situ hybridization in a 2.5-day avian embryo showing high levels of expression in the isthmus and transient domains in branchial arches (black arrowhead) in a control embryo (B) and in a grafted embryo (C) 24 hours after transposition of the isthmus in place of r4 (*). (**D** and **E**) In comparison to a control embryo [(D), white arrow], *Hoxa2* is not expressed in grafted isthmus tissue or in migrating neural crest cells derived from the graft [(E), white arrows]. (**F**) DiI lineage tracing shows that despite the lack of *Hoxa2* expression, there is extensive migration of neural crest cells from the graft into the second arch (white arrow). ba2, second branchial arch.

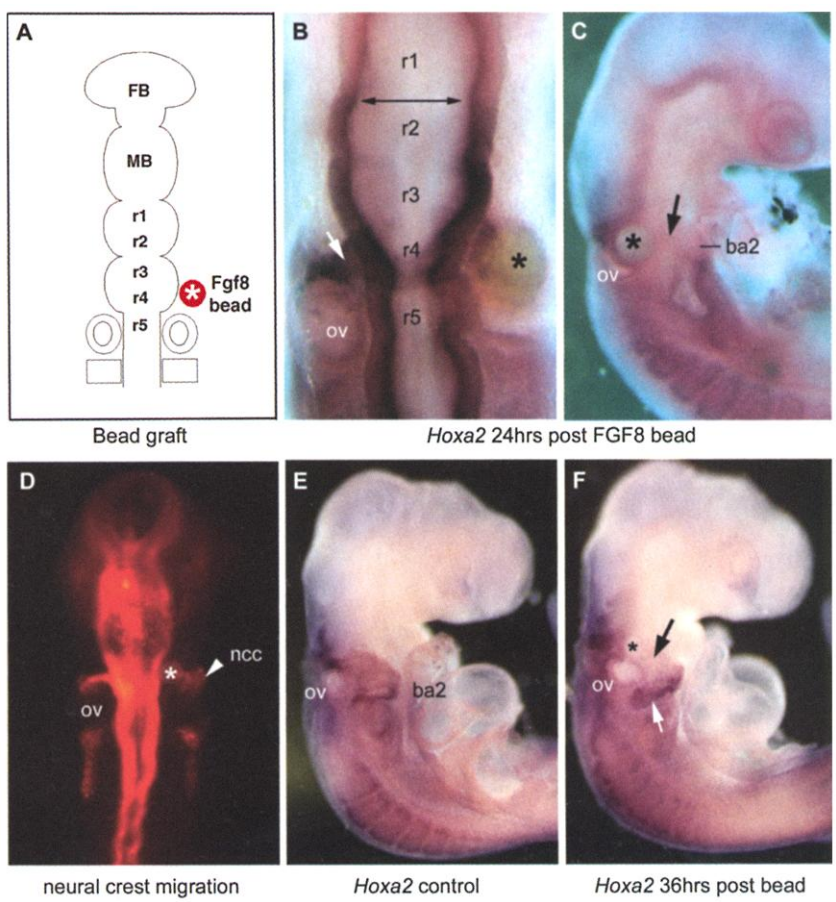

Fig. 2. Transposition of FGF8 beads adjacent to r4 transiently reprograms *Hoxa2* expression in cranial neural crest cells. (**A**) Diagram showing the strategy of placing an FGF8-soaked bead (red circle) next to r4 to examine its effects on neural crest cells. (**B** and **C**) Dorsal view of an embryo (B) 24 hours after transposition with an FGF8 bead (*), showing inhibition of *Hoxa2* expression in second branchial arch (ba2) neural crest cells on the graft as compared to the control side (white arrow). The bead does not alter the anterior limit (double black arrow), segmental domains, or relative levels of expression in the hindbrain. Lateral view of the same embryo (C) showing a complete inhibition of *Hoxa2* expression in second branchial arch neural crest cells (black arrow). (**D**) Lineage tracing of r4-derived neural crest cells showing that the bead does not prevent neural crest cell migration into the second branchial arch (white arrowhead). (**E** and **F**) Lateral views of a control embryo (E) and one containing an FGF8 grafted bead (F) 36 hours after grafting, showing that *Hoxa2* expression is inhibited in the vicinity of the bead [black arrow, (F)] but is reestablished in arch mesenchyme cells distal to the bead [white arrow, (F)].

graft-derived neural crest cells emigrated and populated the second branchial arch (Fig. 1F). The inhibition of *Hoxa2* expression by the isthmus is important because the targeted inactivation of *Hoxa2* results in homeotic transformations of second-arch neural crest derivatives into proximal first-arch derivatives, in a manner similar to that seen in the classic Noden transplantations (*13*, *14*). *Hoxa2* therefore is essential for regulating proper patterning of neural crest–derived skeletal structures in the second branchial arch (*13*, *14*, *25*).

The patterning abilities of the isthmus have been attributed in part to FGF8 (*26*, *27*), which is also transiently expressed in the branchial arches during the early phase of neural crest migration (Fig. 1B). We confirmed that the isthmic territory we transplanted expresses FGF8 (Fig. 1C). Hence, we tested the long-term effects of FGF8 alone on *Hoxa2* gene expression in cranial neural crest cells by placing FGF8-soaked beads (1 mg/ml) into the mesenchymal tissue adjacent to r4, in 8-9 somite stage chick embryos (Fig. 2A). After 24 hours of in ovo culture, *Hoxa2* expression in r4-derived neural crest cells was repressed throughout the entire second branchial arch (Fig. 2, B and C). DiI lineage tracing confirmed that the absence of *Hoxa2* expression was not due to a failure of neural crest cells to migrate into the second arch (Fig. 2D). In contrast to second-arch neural crest cells, FGF8-soaked beads did not affect the levels or segmental boundaries of *Hoxa2* expression in the hindbrain relative to the control side (Fig. 2B). Hence, the repression of *Hoxa2* expression in the neural crest occurs independently of events in the neural tube (Fig. 2, B and C). This is in agreement with ectopic expression studies indicating that *Hoxa2* activation in the migrating neural crest, as opposed to the neural tube, is required for generation of skeletal transformations (*28*, *29*). Together these results show that *Hoxa2* expression is essential for normal patterning of second-arch neural crest cells and is sensitive to the isthmus and FGF signaling.

This suggests that signals from the isthmus, presumably involving FGF8, are capable of inhibiting *Hoxa2* expression, allowing second-arch crest cells to adopt a first-arch fate. If the inclusion of the isthmus accounts for the transformations used to support the prepatterning model, then identical grafts excluding this territory should not result in duplications of first-arch skeletal structures. Therefore, we transposed the anterior hindbrain, with or without the isthmus, in place of the r4 territory at 8-9 somite stage (Fig. 3, A and C). After in ovo embryo culture for 8 days, we assayed for the long-term phenotypic effects in skeletal morphology associated with suppression of *Hoxa2* expression in second-arch neural crest cells by alcian blue staining (Fig. 3, B and D). In grafts containing the isthmus, there was a loss of normal r4-derived second-arch structures, such as the retroarticular process, and in their place the quadrate and Meckel's cartilage characteristic of the first arch were duplicated (Fig. 3, A and B). The embryos were assayed before bone formation, so we could not assess whether the articluar and squamosal bones were also duplicated. However, ectopic cartilage nodules were observed in these relative locations in addition to the duplicated quadrate and Meckel's cartilages. These homeotic transformations are similar to Noden's observations (*2*) and phenotypes observed in *Hoxa2* mutant embryos (*13*–*15*). In contrast, grafts of the anterior hindbrain lacking the isthmus resulted in normal skeletal morphology (Fig. 3, C and D).

These findings demonstrate that the transformation of second-arch crest derivatives into first-arch structures, as described by Noden (*2*), is dependent on the presence of the isthmus. This suggests that the classical first-arch skeletal duplications arising through transpositions of first-arch and frontonasal neural crest (*2*) were a consequence of the suppression of *Hoxa2* expression in the second arch by the isthmus. Therefore, we tested whether FGF8 alone could substitute for the isthmus. However, embryos in which FGF8-soaked beads were grafted into the mesenchyme adjacent to r4 and cultured for 8 days failed to generate duplicated first-arch skeletal elements. This implies that FGF8 alone in this context is unable to replace the isthmus, suggesting that additional factors may also be involved. This prompted us to examine the temporal effects of FGF8 beads on *Hoxa2* expression in the second branchial arch. We found that as the arch grows over time (36 to 48 hours), *Hoxa2* expression is reestablished in the arch mesenchyme at a distance from the bead, but it continues to be inhibited in cells adjacent to the bead (Fig. 2, E and F). Hence, in contrast to isthmic grafts, FGF8 beads only transiently inhibit *Hoxa2* expression in the second arch. This result reflects an important difference in the nature of isthmus/tissue versus bead transplantations. In grafts of the isthmus, the entire endogenous presumptive r4 crest was removed and replaced with the FGF8-expressing isthmus. However, in bead grafts, the endogenous r4 crest was left intact, and migrating crest cells derived from r4 are being challenged to reprogram by signals from the grafted bead. These experimental properties, in combination with the transient inhibition of *Hoxa2* expres-

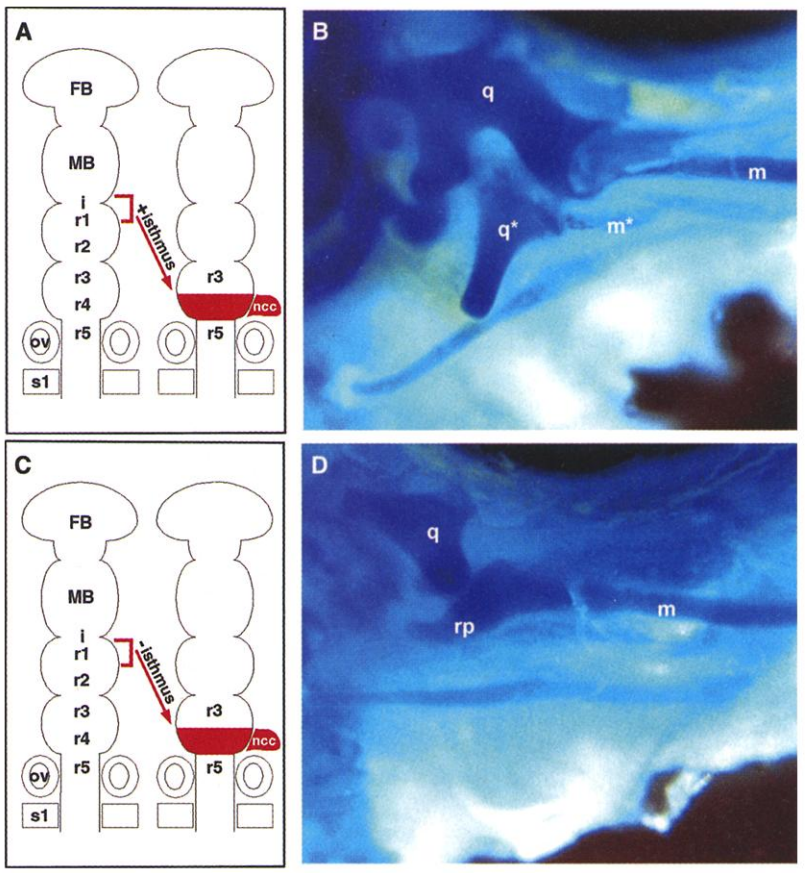

Fig. 3. Skeletal analysis of grafted embryos containing hindbrain transpositions including or excluding the isthmus. (**A**) Diagram illustrating the posterior transposition of r1 and the isthmus to r4. (**B**) The posteriorly transposed isthmus/r1 results in duplication of first-arch skeletal structures such as the quadrate (q*) and Meckel's cartilage (m*) and loss of the retroarticular process (rp). (**C**) Diagram illustrating the posterior transposition of r1 excluding the isthmus to r4. (**D**) The first-arch skeletal morphology, including Meckel's cartilage (m) and the quadrate (q), is normal.

sion, could well account for the differences in skeletal phenotypes between isthmus and FGF8 bead grafts. Therefore, the variability in the duplications observed by Noden may also be explained by the variability of local FGF8 concentration present in grafted tissue. In contrast to the isthmic grafts, the duplicated first-arch structures observed in the *Hoxa2* mutants exhibit a mirror image polarity. This implies that other factors must be involved in patterning different axes of polarity in these duplications. The transposition of a signaling center might disrupt the mechanisms that influence polarity or axis patterning.

These experiments underscore the important role played by *Hoxa2* in branchial arch identity. Recently, functional inroads have been made into understanding the precise mechanisms by which *Hoxa2* influences the morphogenesis of second-arch elements (*30*). *Hoxa2* is widely expressed in the second-arch mesenchyme but is excluded from the chondrogenic domains and acts very early in the chondrogenic pathway upstream of *Sox9*, *Col2a1*, and *Cbaf11* to repress their expression. During normal development, both endochondral and dermal (intramembranous) ossification occurs in first-arch morphogenesis; however, endochondral ossification primarily occurs in second-arch morphogenesis. Therefore, one of the roles of *Hoxa2* in the second branchial arch may be the prevention of dermal bone formation. Overexpression studies of *Hoxa2* in chick and zebrafish embryos have now confirmed its role as a true selector gene (*28*, *29*). Therefore, *Hoxa2* not only inhibits development of the lower jaw skeleton but is also primarily responsible for specifying second branchial arch fate.

The presence of the isthmus as a mechanistic basis for first-arch duplications also helps resolve two puzzling aspects of Noden's work (*2*). First, there was considerable variability in the frequency of duplications observed, presumably arising through variable inclusion of the isthmus and, consequently, the local concentration of FGF8. Second, it explains why both first-arch and frontonasal neural crest develop similar duplicated skeletal structures when transposed posteriorly, even though they are derived from different axial levels.

Therefore, rather than providing evidence for the prepatterning of neural crest cells, Noden's experiments (*2*) highlight the importance and effects of local signaling centers, such as the isthmus, in A-P patterning and regulation of *Hox* gene expression (*26*, *27*). This study, together with recent evidence from mouse, chick, and zebrafish transplantation studies, argues as a general principle that cranial neural crest cells are not prespecified or irreversibly committed before their emigration from the neural tube (*5*, *11*, *16*–*18*). Rather, neural crest patterning is based on plasticity and the ability of neural crest cells to respond to environmental influences in the branchial arches, and future attention will be focused on the nature of these signals.

References and Notes

1. N. Le Douarin, *The Neural Crest* (Cambridge Univ. Press, Cambridge, 1983).
2. D. Noden, *Dev. Biol.* **96**, 144 (1983).
3. ———, *Development* **103**, 121 (1988).
4. A. Lumsden, R. Krumlauf, *Science* **274**, 1109 (1996).
5. P. Trainor, R. Krumlauf, *Nature Rev. Neurosci.* **1**, 116 (2000).
6. A. Lumsden, N. Sprawson, A. Graham, *Development* **113**, 1281 (1991).
7. G. Serbedzija, S. Fraser, M. Bronner-Fraser, *Development* **116**, 297 (1992).
8. J. Sechrist, G. N. Serbedzija, T. Scherson, S. E. Fraser, M. Bronner-Fraser, *Development* **118**, 691 (1993).
9. N. Osumi-Yamashita, Y. Ninomiya, H. Doi, K. Eto, *Dev. Biol.* **164**, 409 (1994).
10. T. F. Schilling, C. B. Kimmel, *Development* **120**, 483 (1994).
11. P. M. Kulesa, S. E. Fraser, *Development* **127**, 1161 (2000).
12. P. Kulesa, M. Bronner-Fraser, S. Fraser, *Development* **127**, 2843 (2000).
13. F. M. Rijli *et al.*, *Cell* **75**, 1333 (1993).
14. M. Gendron-Maguire, M. Mallo, M. Zhang, T. Gridley, *Cell* **75**, 1317 (1993).
15. O. Chisaka, M. Capecchi, *Nature* **350**, 473 (1991).
16. T. Schilling, *Dev. Biol.* **231**, 201 (2001).
17. P. Trainor, R. Krumlauf, *Nature Cell Biol.* **2**, 96 (2000).
18. J. Saldivar, C. Krull, R. Krumlauf, L. Ariza-McNaughton, M. Bronner-Fraser, *Development* **122**, 895 (1996).
19. J. R. Saldivar, J. W. Sechrist, C. E. Krull, S. Ruffin, M. Bronner-Fraser, *Development* **124**, 2729 (1997).
20. P. Hunt, J. D. W. Clarke, P. Buxton, P. Ferretti, P. Thorogood, *Dev. Biol.* **198**, 82 (1998).
21. G. F. Couly, A. Grapin-Bottom, P. Coltey, N. M. Le Douarin, *Development* **122**, 3393 (1996).
22. N. Itasaki, J. Sharpe, A. Morrison, R. Krumlauf, *Neuron* **16**, 487 (1996).
23. A. Grapin-Botton, M.-A. Bonnin, L. Ariza-McNaughton, R. Krumlauf, N. M. LeDouarin, *Development* **121**, 2707 (1995).
24. A. L. Joyner, *Trends Genet* **12**, 15 (1996).
25. G. Couly, A. Grapin-Botton, P. Coltey, B. Ruhin, N. M. Le Douarin, *Development* **128**, 3445 (1998).
26. P. Crossley, G. Minowada, C. MacArthur, G. Martin, *Cell* **84**, 127 (1996).
27. C. Irving, I. Mason, *Development* **127**, 177 (2000).
28. M. Pasqualetti, M. Ori, I. Nardi, F. M. Rijli, *Development* **127**, 5367 (2000).
29. G. A. Grammatopoulos, E. Bell, L. Toole, A. Lumsden, A. S. Tucker, *Development* **127**, 5355 (2000).
30. B. Kanzler, S. J. Kuschert, Y.-H. Liu, M. Mallo, *Development* **125**, 2587 (1998).

31. The authors are grateful to A. Issacs and C. Tickle for providing beads and FGF8 and to P. Cambronero, N. Itasaki, D. Ellies, T. Inoue, M. Bronner-Fraser, S. Fraser, and P. Tam for helpful discussions. Funded by Core Medical Research Council and Stowers Institute support for R.K. and P.A.T., and a Human Frontiers in Science Program research grant (RG0146/2000-B) with R.K. as principal coordinator.

18 July 2001; accepted 11 January 2002

MAPKK-Independent Activation of p38α Mediated by TAB1-Dependent Autophosphorylation of p38α

Baoxue Ge,[1] Hermann Gram,[2] Franco Di Padova,[2] Betty Huang,[3] Liguo New,[1] Richard J. Ulevitch,[1] Ying Luo,[3,4] Jiahuai Han[1]*

Phosphorylation of mitogen-activated protein kinases (MAPKs) on specific tyrosine and threonine sites by MAP kinase kinases (MAPKKs) is thought to be the sole activation mechanism. Here, we report an unexpected activation mechanism for p38α MAPK that does not involve the prototypic kinase cascade. Rather it depends on interaction of p38α with TAB1 [transforming growth factor-β–activated protein kinase 1 (TAK1)–binding protein 1] leading to autophosphorylation and activation of p38α. We detected formation of a TRAF6-TAB1-p38α complex and showed stimulus-specific TAB1-dependent and TAB1-independent p38α activation. These findings suggest that alternative activation pathways contribute to the biological responses of p38α to various stimuli.

Mitogen-activated protein kinases (MAPK) have crucial roles in cellular responses to various extracellular signals (*1*). The prototypical module of MAP kinase activation is a cascade of three kinases, consisting of MAP3K (MAP kinase kinase kinase), MAPKK, and MAPK (*2*). p38α is a MAPK activated by MAPKKs MKK3 and MKK6 (*2*–*7*). Although the protein kinase cascade is unquestionably a mechanism controlling p38α activation (*2*–*7*), we have identified an alternative p38α activation mechanism that has not previously been addressed.

We used the yeast two-hybrid system with a library constructed from human gastrointestinal tract tissue to search for proteins that

[1]Department of Immunology, The Scripps Research Institute, 10550 North Torrey Pines Road, La Jolla, CA 92037, USA. [2]Novartis Pharma AG, CH-4002, Basel, Switzerland. [3]Rigel, Inc., South San Francisco, CA 94080, USA. [4]Shanghai Genomics, Inc., Shanghai, China.

* To whom correspondence should be addressed. E-mail: jhan@scripps.edu